THE PENNSYLVANIA STATE UNIVERSITY
SCHREYER HONORS COLLEGE

DEPARTMENT OF CHEMICAL ENGINEERING

ELECTRON TRANSFER THROUGH PHOTOSYSTEM I MEMBRANE PROTEINS WITH BLOCK COPOLYMER INTERFACES

EMELIA CONTE
SPRING 2018

A thesis
submitted in partial fulfillment
of the requirements
for a baccalaureate degree
in Chemical Engineering
with honors in Chemical Engineering

Reviewed and approved* by the following:

Manish Kumar
Associate Professor of Chemical Engineering
Thesis Supervisor

Scott T. Milner
Joyce Chair and Professor of Chemical Engineering
Honors Adviser

* Signatures are on file in the Schreyer Honors College.

ABSTRACT

Renewable energy, particularly solar energy, has been gaining traction as a more widely used energy source in recent years due to increased world energy usage and decreasing cost of renewable technologies. However, currently manufactured solar devices suffer from low solar conversion efficiency and can be costly to produce, resulting in the emergence of research of bio-photovoltaic and organic solar cells due to their low manufacturing cost. This project aims to develop a photosystem I (PSI)/block co-polymer (BCP) integrated membrane intercalated with conductive oligoelectrolytes that can interface with a conductive electrode for increased solar conversion efficiency and stability compared to current bio-photovoltaics. It is important to develop organic photovoltaic systems with the ability to produce high photocurrents to create a low-cost system capable of producing enough energy to contribute to the world's need for renewable energies. In this study, PSI-BCP membranes are assembled on an electrode surface and tested for photocurrent production and device longevity. Some of the highest reported photocurrents for similar organic and bio-photovoltaics compared to current literature, up to 35.0 ± 3.5 μA cm^{-2}, were generated from PSI-BCP devices, which showed stable photocurrent generation for at least one month. These findings exhibit that photo-active BCP-protein integrated membrane structures have potential for use in solar energy conversion, as well as for sensing applications for biomedical devices.

TABLE OF CONTENTS

LIST OF FIGURES

ACKNOWLEDGEMENTS

I would like to thank Dr. Manish Kumar for his immense guidance during my undergraduate research at Penn State, and for providing me with opportunities to enhance my research capabilities throughout my time as an undergraduate. The Kumar group at the Pennsylvania State University, especially Patrick Saboe, were instrumental in the completion of this thesis research. I would also like to thank my honors advisor, Dr. Scott T. Milner, for his assistance throughout my undergraduate career. Thanks to the various organizations that have provided financial support for my education, including Pittsburgh Plate Glass Inc. through the National Merit Scholarship Corporation, The Pennsylvania State University, and the Pennsylvania Space Grant Consortium. Finally, a special thank you all of my friends, peers, and family members who have supported my throughout my time at Penn State.

Chapter 1

Problem Statement

The search for alternative energy sources has been a major concern across disciplines. A study done by J.G. McGowan identified that the need for renewable energy sources is based on contributing factors including major environmental problems, environmental degradation, depletion of the world's nonrenewable energy sources, and increasing energy use in developing countries.[1] In particular, the United States has steadily increased their use of renewable energy in past years. As of March 2016, about 9.9 percent of all energy consumed in the U.S. was from renewable sources, with petroleum and natural gas contributing to the majority of energy consumption with 36.2 percent and 29 percent use, respectively.[2] The usage of renewable energy sources is expected to increase in the next decades, primarily due to falling cost of solar and wind energy.[3] These falling prices are driven by the need for more cost effective renewable energy sources to combat the effects of global warming. Renewables will need to account for 42 percent of electricity use in 2030 and 57 percent in 2050 to keep within a 2 ℃ global warming threshold.[3] To accommodate for this increasing need for renewable energy, scientists and engineers are creating more efficient and less expensive means of large scale renewable energy harvesting.

1.1 Traditional solar cells for renewable energy

Solar panels are perhaps the most well-known renewable energy source in use today. Despite the name recognition associated with this technology, traditional solar panels only

contributed to 5 percent of renewable energy consumption in 2015.[2] However, the projected falling costs of solar energy by 47 percent by 2040 will make this technology a large contributor to the world's energy use in coming decades.[3] Solar panels frequently operate using an electric field created by seeding negatively charged phosphorous on the top silicon layer of the panel and positively charged boron on the bottom silicon layer.[4] The panel then generates electricity by harvesting photons from a light source and using the photons to excite and eject electrons from the silicon panel (**Figure 1**, below).[4] Making solar panels efficient and inexpensive enough to compete on the global market has been a challenge for some time. Although Japanese researchers have set an efficiency record of 26.6 percent for mass-produced solar panels,[5] most commercial panels only have a maximum efficiency of 15 percent,[6] necessitating additional research to create more efficient solar cells that have the potential for large scale solar energy conversion.

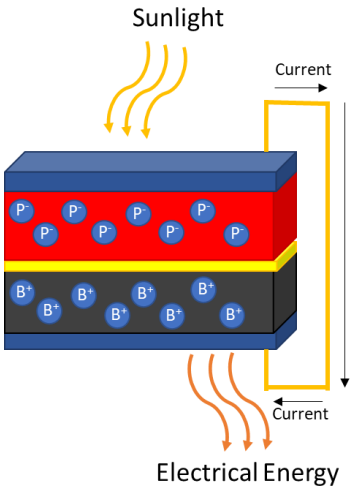

Figure 1. Schematic of commercial solar panel. Doping with negatively charged phosphorus ions and positively charged boron ions promotes electron transfer from top to bottom upon introduction of sunlight to produce electrical energy.

1.2 Current research – organic photovoltaics

Many researchers have focused on increasing the efficiency of traditional silicon solar cells while keeping them at a low cost for consumers. However, these cells are still limited by their inherently low efficiencies and relative high cost compared to commonly used energy sources. Some research explores organic and bio-photovoltaic cells as a contrast to traditional silicon or hard material solar cells. Specifically, bio-photovoltaic cells using self-assembling crystals of light-harvesting photosystem I membrane proteins on a lipid bilayer to produce light energy have gained traction in recent years. Since the photosystem I proteins function naturally in plant cells to convert light energy into energy in the form of excited electrons,[7] the protein works as a perfect analog to the function of traditional solar panels. Recently, Saboe et al. created such two-layered cells that produced four times more photocurrent than monolayered cells commonly used for this field of research.[8] Although these lipid membranes are becoming increasingly efficient, they are also highly susceptible to degradation through oxidation, making their commercial use currently infeasible.

Chapter 2

Background and Hypothesis

To alleviate the issues presented by a fully bio-photovoltaic cell, the integration of synthetic polymer elements, or block copolymers (BCPs), into these systems has been investigated. These BCPs would replace the lipid bilayer in the photosystem I (PSI) crystals to create an organic, more efficient, less expensive photovoltaic. Based on the ability of BCPs to mimic native lipid environments, their conductive capabilities, and their stability over time, the replacement of lipid bilayers with BCPs in current bio-photovoltaics is likely to provide a stable system with enhanced photocurrent capabilities compared to currently explored bio-photovoltaics to allow for increased lifetime of the cells.

2.1 Overview of block copolymer use in organic photovoltaics

Block copolymers (BCPs) are synthetic molecules made from linking together multiple types of different monomers in organized "blocks" that prevent the monomer types from intermingling.[9] These BCPs can be synthesized by researchers to have a wide variety of specialized properties, including enhanced conductivity and rigidity.[10] Their unique properties allow BCPs to have proposed uses in multiple areas of science and engineering, including uses in photovoltaic research.

Both bio-photovoltaic lipid and organic BCP photovoltaic cells have the same general structure; a gold electrode supports a bilayer consisting of a tethering self-assembled monolayer (SAM) and collapsed vesicles. Next, photosystem I proteins integrated into a lipid or BCP membrane are placed on top of the stable bilayer. In both cases, conjugated oligoelectolytes

(COEs) are included in the bottom bilayer of lipid or BCP. On their own, lipids and BCPs are poor conductors of electrons, reducing the ability of the cell to conduct electrical current. Including molecules of conductive COE allows for greater electron transfer through the membrane, resulting in increased current through the devices. **Figure 2**, below, indicates differences in structure of a lipid bilayer supported versus a BCP supported photovoltaic cell. The specific molecules depicted are subject to modification based on the needs of the project.

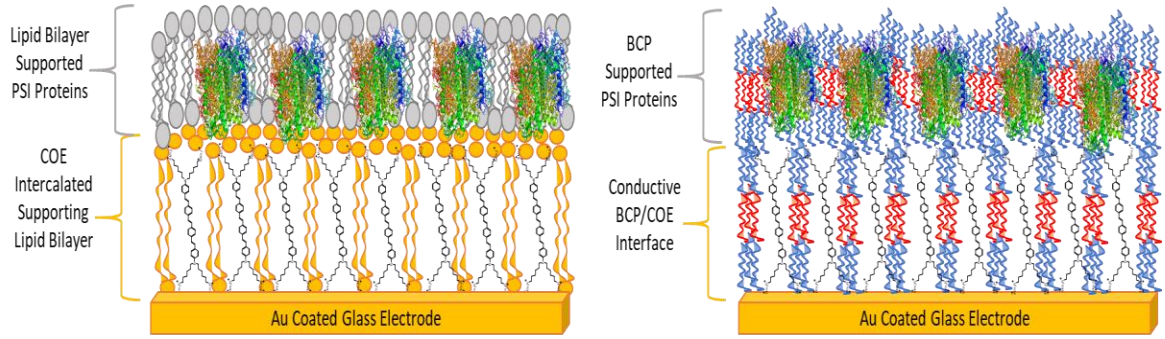

Figure 2. Comparison of lipid bilayer supported photovoltaic to block copolymer photovoltaic system. The general bilayer supported protein structure is maintained in both systems.

The major difference between lipid bio-photovoltaics and organic BCP photovoltaics is the compound used to create the bilayer and protein membranes. In the more commonly tested lipid bio-photovoltaics, the bilayer and protein-integrated membrane are formed from lipid molecules found in the protein's native environment. The bilayer in these systems is a tethered lipid bilayer membrane (tBLM) analogous to biological cell membranes. tBLMs allow embedded enzymes to preserve their functionality but can introduce constraints on bilayer diffusion and protein conformation, potentially preventing enzymes from undergoing conformational changes necessary to their function in the membrane.[11, 12] In contrast, organic BCP photovoltaics use BCPs with specifically tailored properties that mimic those of lipids in the protein's native environment to create the bilayer and protein-integrated membrane system. The membrane

system in the BCP scenario provides additional protection from surface interactions,[13] and their ability to cross-link provides a more stable and compatible environment for membrane proteins as compared to tBLM systems.[14] It is the difference in the conductivity of these lipid bio-photovoltaics and BCP photovoltaics that is crucial to differentiating the BCP photovoltaics against traditional lipid bio-photovoltaics.

2.2 Mimicking biological environments with block copolymers

The development of biological membranes in natural cell environments is a common occurrence. Thus, a synthetic membrane that forms in a similar manner to these natural biological membranes can effectively mimic their natural environment. Most lipid membranes form due to hydrophilic-hydrophobic interactions between lipid molecules, which is fundamental to determining the function of proteins within that membrane. A balance of structurally hydrophilic-lipophilic interactions between lipid heads and tails can be mimicked by BCPs through self-assembly, and it has been shown that this contributes to their ability to form cell-like membranes and vesicles as depicted in **Figure 3**, below.[15] BCPs can be tailored with additional factors, like slower chain dynamics and the polydispersity of molecular weight, to more accurately represent the formation of biological membranes and provide specificity to the specific membrane researchers wish to replicate.[15] Researchers have used a large quantity of BCP samples with different properties to derive complex mathematical models for the general integration of proteins into BCP membranes, showing a high success rate.[16]

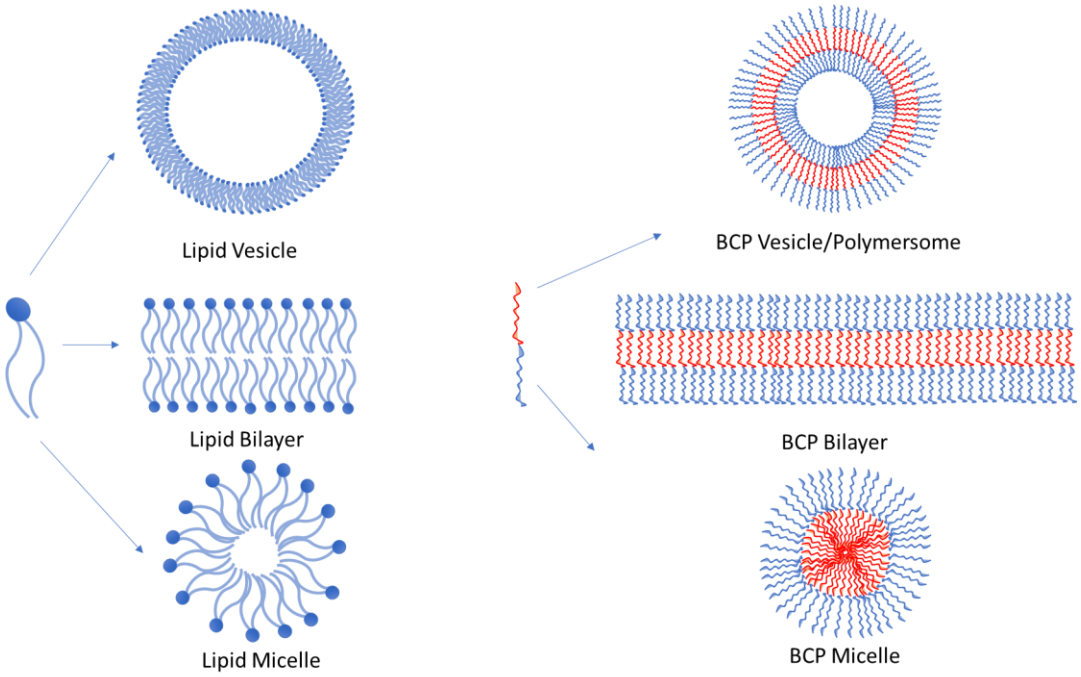

Figure 3. Mechanisms for lipid and block co-polymer formation in biological systems.

Some aspects of the mechanism of self-assembly have raised concern; although BCP membranes reportedly arrange themselves much like biological membranes when left to themselves, there are some occasions in which their formation does not go exactly as planned. Reports can be found that perylene bismide results in the formation of extremely large crystals with poor morphological control when left to self-assemble.[17] These conditions are not ideal for membrane conduction, since thinner membranes provide more stability for the proteins. While this BCP is one that can be used by researchers to understand where to exercise caution in the use of self-assembled BCPs, only few occurrences of undesirable effects have been reported, and most research shows that there are more synthetic polymers that can be created with unique properties that guide their formation.[15] BCPs largely direct themselves based on their molecular makeup, so self-assembly can be constrained by tailoring the BCP with molecules which give it the desired assembly properties to avoid poor membrane morphology.[15]

Because PSI proteins must be able to survive in the BCP membrane for elongated periods of time, it is critical to ensure that the synthetic membrane does not hinder the functionality of the proteins. Recently, uses of synthetic BCPs to induce spontaneous reconstitution of photosynthetic proteins to form membranes coupled with 2D crystals have shown that thick BCP integrated membranes can be formed that successfully retain the functionality of photosynthetic proteins.[18] This means that synthetic and biological materials can be integrated successfully, and that these synthetic materials do have the potential to mimic the natural environment.

2.3 Conducting current through block copolymer membranes

BCPs are easily customized for use by researchers, resulting in many variations of electrical conductivity of their membranes. Although there are multiple conductive morphologies of BCPs, when vertically aligned, uncharged BCPs provide a clear pathway for electrons to travel from the electrode surface to proteins on the membrane surface.[19] In the proposed application of BCPs with intercalated conductive COEs, vertically aligned BCPs facilitate the alignment of COE molecules to essentially form a ladder from the electrode to the proteins to provide for the most efficient transfer of electrons. Morphologies in which BCPs and COEs are not vertically aligned can result in fewer continuous paths that connect the electrode surface directly to a photosystem protein, potentially causing a loss of efficiency in converting photons to usable energy (**Figure 4**, below). Because lack of commercial efficiency is one of the primary detriments of solar panels currently on the market, configurations that maximize electrical efficiency are most desirable. Although aligning BCPs normal to the plane of the electrode can prove challenging due to the effect of interfacial interactions, mathematical models using an applied electric field in cylindrically arranged units of BCPs to ensure that they remain in the

desired conductive configuration have been developed.[19] BCPs can arrange themselves into units with a variety of morphologies which are capable of responsivity to electric fields and that can be modified for electron transport. Multiple morphologies of BCPs, including cylindrically arranged BCP units and bulky BCP crystals are excellent candidates for harvesting light.[17]

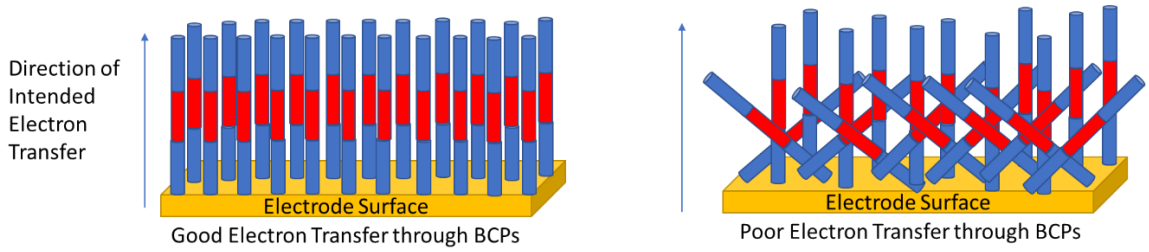

Figure 4. Comparison of cylindrically arranged BCP units for electron transfer through a BCP COE-intercalated membrane. When BCPs and COEs are misaligned, electron transfer cannot occur efficiently because the paths for electron travel are not all direct and continuous from the electrode to the protein.

Likewise, the combination of BCP membranes and proteins like PSI has proven successful at generating current through devices. Integrated BCP and protein interfaces have helped researchers gain the understanding that these interfaces are conductive, and that the electron transfer properties are largely insensitive to variations in the molecular makeup of BCP membranes.[18] Some occurrences of such integrated interfaces including BCPs with integrated Rhodobacter sphaeroides RC proteins have exhibited photocurrent generation,[18] paving the way for systems that increase electron transport.

Despite the ability of synthetic membranes to stabilize membrane proteins, BCP membranes typically have low dielectric constants, which can prevent layers of integrated membrane proteins from accessing electrical contact with the electrode.[20] For this reason, tBLM or BCP membranes can also integrate conjugated oligoelectrolytes (COEs) in membranes to create a pathway for electrons through the membrane, resulting in increased electron transfer between the electrode and the integrated membrane proteins. COEs integrate themselves into a

specific orientation in a lipid bilayer that allows for the best electron transfer across the membrane; their natural configuration is perpendicular to the plane of the membrane, shown in **Figure 5**.[21] Recently, COEs have been integrated into bio-photovoltaic membrane interfaces that have shown electrical conduction far superior to systems without COE molecules.[8] Such studies provide evidence that the inherent conductivity of BCPs can be enhanced even further using similar conductive molecules to provide increased performance of photovoltaics.

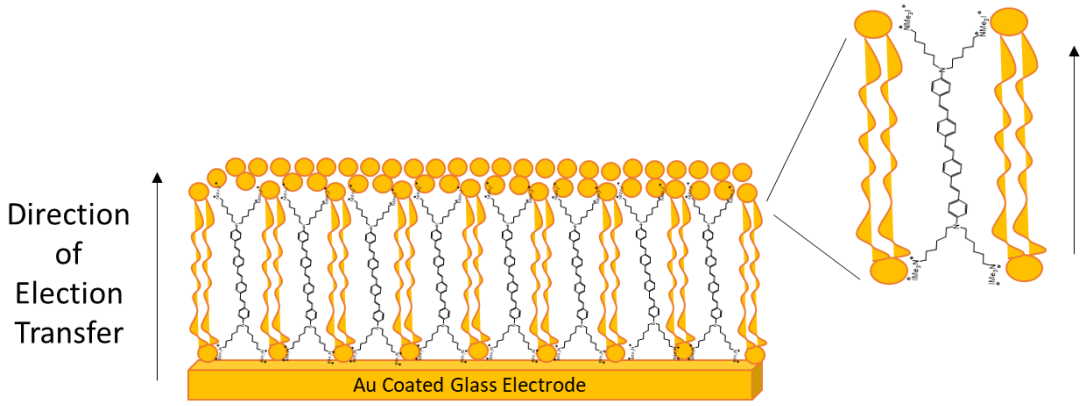

Figure 5. Proper orientation of a conjugated oligoelectrolyte (COE) in a lipid bilayer.

2.4 Stability of the block copolymer membrane

It is crucially important to ensure the enhanced stability of BCPs, since commercial photovoltaics must have enhanced longevity to make them feasible and to gain high public appeal. It has been shown that the incorporation of BCPs into photovoltaic systems result in mechanically more stable membranes and vesicles, and that the stability of BCPs can be manipulated.[22] Specifically, cross-linking stabilizes BCP membranes, with low levels of cross-linking associated with drastic reduction of rupture strength of a membrane and the formation of micropores (**Figure 6**, below). [19]

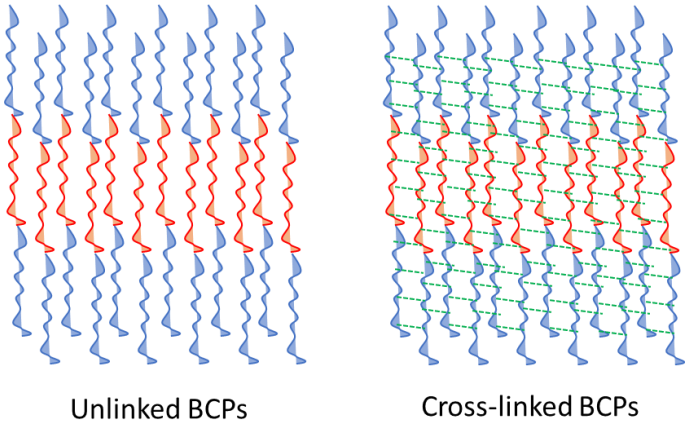

Figure 6. Cross linking enhances the overall stability of BCP membrane systems.

However, some reports exist that propose draw-backs of cross-linking. Conventional cross-linking approaches do solve the issue of BCP stability, but can cause problems by decreasing membrane permeability.[23] Current methods of membrane formation typically use soluble micelles to transport the membrane materials to the photovoltaic cell environment, making this conclusion detrimental to these methods. However, several alternative methods of cross-linking BCPs can be found in the literature that result in unique tradeoffs between system stability and membrane permeability, allowing researchers to choose a cross-linking procedure that best fits their needs for the desired system.

2.5 Hypothesis

The goal of this research is to develop a PSI-BCP membrane intercalated with COEs that can interface with a conductive electrode. A cross-linked system will also be analyzed to prove that the stability of the system can be increased without a corresponding loss of electron transfer activity. This device would have numerous applications, including for use as a solar energy

harvesting organic photovoltaic for electrical power, due to its enhanced stability, ability to produce high currents, and integration of biological and synthetic components.

Previous experimentation by Saboe et al. has shown that PSI proteins self-assemble into ordered 2D crystals in artificial lipid membranes, and that COEs can be incorporated to give a 4-fold increase in photocurrent as compared to unmodified tBLM systems and PSI monolayers on self-assembled monolayers (SAMs).[8] The next step based on these findings is to prove that PSI proteins can be incorporated into BCP composite membranes with COE intercalation, and that this system provides enhanced stability and conductivity compared to the PSI-COE intercalated tBLM system. Specifically, the poly(butadiene)$_{12}$-poly(ethylene oxide)$_8$ (PB_{12}-PEO_8) BCP will be used to form a highly packed composite membrane due to its ability to mimic the bilayer formation of lipids.[24] Likewise, the COE 4,4'-bis(4'-(N,N-bis(6"-(N,N,N-trimethylammonium)hexyl)amino)-styryl)stilbene tetraiodide (DSSN+) (**Figure 7**) is used because of its ability to be incorporated into membranes and to provide enhanced electron transfer from the electrode through the membrane to the PSI proteins.[8, 25] These elements should combine into a PSI-BCP integrated membrane with increased photocurrent and stability.

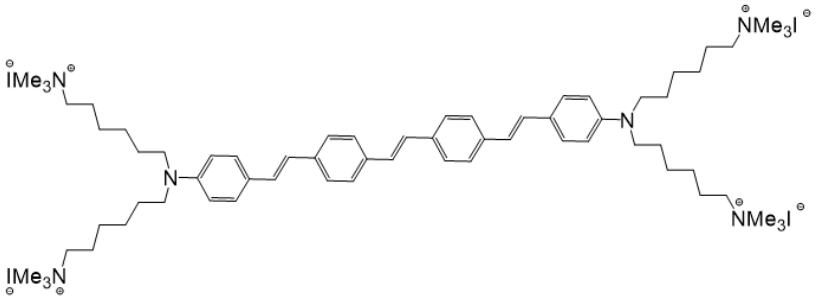

Figure 7. The structure of the conjugated oligoelectrolyte, DSSN+. The molecule can easily integrate into biological membranes to provide enhanced electron transfer.

Chapter 3

Materials and Methods

This thesis research aims to develop a PSI-BCP membrane intercalated with DSSN+ that produces photocurrent quantifiable by single potential time base voltammetry, a technique that applies a voltage across the cell and measures the current as a function of time across the voltage. Creation of the membrane is a dynamic process involving assembly of the PSI-BCP membrane, deposition on prepared electrode surfaces, and photoelectrochemical testing of the system. In addition to independently characterizing the electron transfer properties of the system, its longevity compared to systems without integrated BCP is also investigated.

3.1 Block copolymer-Photosystem I membrane assembly

PSI and PsaL deficient *PsaJ*-his_6-tagged PSI was isolated from *Synechococcus sp.* PCC 7002 through treatment with 1% Triton X-100 followed by ultracentrifugation to remove the PSI complex. PSI was removed from the complex with 6.8 M urea.[26] For reconstitution, PSI was size excluded and precipitated with PEG6000/$MgCl_2$ and was resuspended in 0.5% *n*-octyl-β,D-thioglucoside (OTG) and 10 mM HEPES pH 7.0.[27] Poly(butadiene)$_{12}$-Poly(ethylene oxide)$_8$ (PB_{12}-PEO_8) with carboxylic acid terminated polyethylene oxide solubilized in 10 wt % OTG was mixed with PSI with PoPR w/w of 0.5-1.0 with a final concentration of 1.0 mg/mL PSI. Detergent concentration was adjusted to 4% and dialyzed against 0.5% OTG buffer of 10 mM MES pH 6.0, 6 g/L ammonium ferric citrate, and 3 mM NaN_3 using dialysis buttons of volume

60 µL at 25 ℃ for 24 hours. Dialysis buttons were then transferred to detergent free buffer for additional dialysis over 72 hours.

3.2 Preparation of electrodes

Glass slides coated with a 5 nm layer of chrome and a 100 nm layer of gold were cleaned using a solution of 3:1 sulfuric acid and 30% hydrogen peroxide (Piranha solution) for 15 minutes. Following submergence in Piranha solution, slides were washed with deionized water and subsequently with ethanol and were dried in a stream of nitrogen gas.

3.3 Cyclic voltammetry of bare gold electrode

Cyclic voltammetry was conducted using an Ag/AgCl reference electrode, a Pt-wire counter electrode, and a gold working electrode. A scan rate of 100 mV s^{-1} from -100 mV to 400 mV was used. The electrolyte solution for the procedure contained 0.5 M KCl, 100 µM $[K_3FeCN_6]^{3-}$, and 100 µ$[K_4FeCN_6]^{4}$.

3.4 Electrode modification

Cleaned gold electrodes were modified with a solution of 0.075 mM tethering PB_{12}-PEO_8 (T-PB) (5 mM stock in chloroform), 0.075 mM PB_{12}-PEO_8 (10 mM stock in chloroform), and 0.3 mM dithiodiglycolic acid (30 mM stock in 100% ethanol) for one hour to form a self-assembled monolayer (SAM). A solution of 0.05 mg/mL of PB-PEO-COOH (6-20), 25 mol % DSSN+, and 5% octyl-beta-glucoside (OG) was then added to the SAM gold electrodes for 48 hours at 25℃.

To remove OG detergent, a dialysis membrane (10-12 kDa cutoff) was added to the electrode. The gold electrode was clamped with an aluminum clamp to a glass O-ring-joint. The dialysis membrane was fit to the glass cell opening with a modified dialysis button and secured with an O-ring. The volume of the set-up was 3 mL. Detergent was removed by placing the cell in 1 L of dialysis buffer made from 100 mM NaCl, 50 mM Tris pH 8.3, and 3 mM NaN_3 for 3 days with a stir bar. Dialysis buffer was changed every 24 hours. After 3 days, the dialysis button was removed and deionized water was used to maintain membrane integrity.

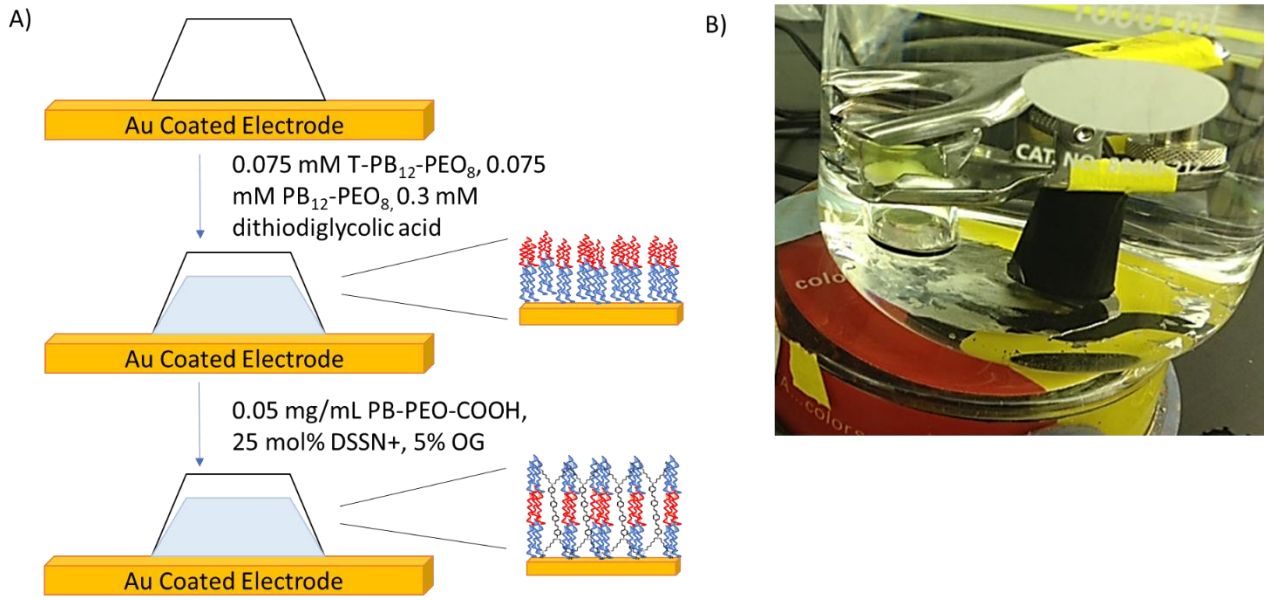

Figure 8. Schematic of BCP self-assembled monolayer (SAM) procedure. A. Assembly of a SAM on a gold electrode. B. Dialysis procedure.

3.5 Photocurrent measurements

PSI/BCP membranes were self-assembled at a PoPR of 0.5-0.8 in 10 mM HEPES pH 7.0, 100 mM NaCl, 10 mM $MgCl_2$, and 3 mM NaN_3 for photocurrent analysis. Reconstitution PSI membranes containing 0.09 mg PSI were deposited onto DSSN+/PB-PEO bilayer modified electrodes of area 2.8 cm^2 (as described in section 3.4). Photoelectrochemical measurements

were completed on tBLMs with intercalated DSSN+ and immobilized PSI crystals on tBLMs and tBLMs with DSSN+ modified gold working electrodes using a BASi potentiostat at room temperature using an Ag/AgCl reference electrode, a Pt-wire counter electrode, and a working electrode bias of 300 mV, a sample interval of 150 msec, run time of 800 sec, and sensitivity of 10 µA/V. The electrolyte solution contained 10 mM MES pH 6.0, 2 mM 1,1'-dimethyl-4,4'-bipyridinium (methyl viologen), 100 µM PMS, 100 µM $K_3[Fe(CN)_6]^{3-}$, 100 µM $K_4[Fe(CN)_6]^{4-}$. Electrodes were illuminated with 100 µmol m^{-2} s^{-1} (400-700 nm) (approximately 20 mW cm^{-2}) of light from an Oriel Type 1958 tungsten lamp. Membranes were prepared for photoelectrochemical measurements by rinsing 10-15 times with deionized water to remove excess bilayer molecules, attaching the positive lead to the Pt-wire counter electrode, the negative lead to the Ag/AgCl reference electrode, and the ground lead to the corner of the gold electrode. The system was allowed to stabilize in the dark, was exposed to tungsten lamp light for 20 seconds, and was allowed to recover in the dark for an additional 20 seconds or more.

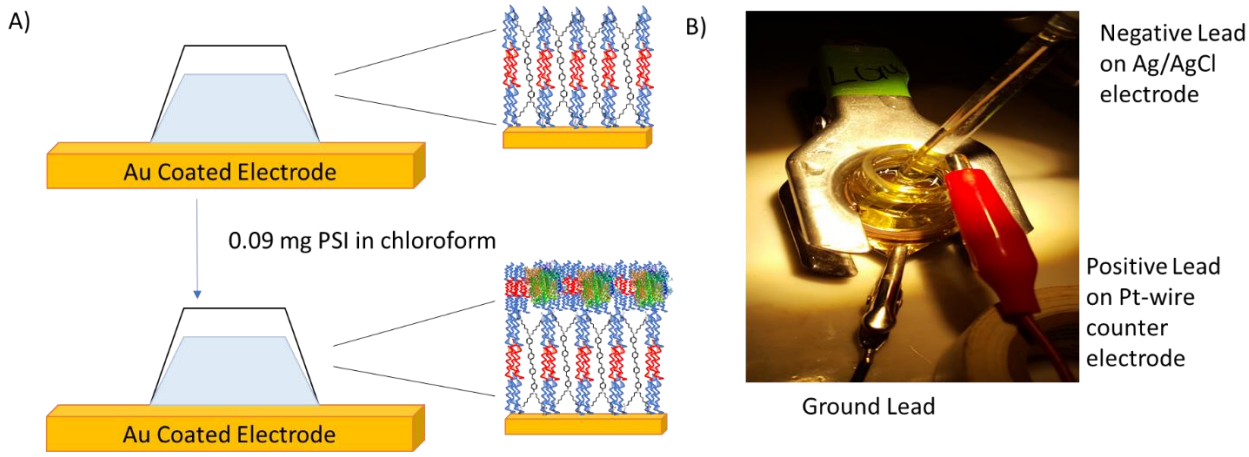

Figure 9. PSI integration and photoelectrochemical testing. A. Procedure for integrating PSI proteins atop the BCP bilayer. B. Setup of electrochemical cell for single base potential voltammetry readings.

3.6 UV-Vis

UV-Vis spectra were measured with a NanoDrop 2000C spectrophotometer between wavelengths of 400 to 700 nm.

3.7 Stability of DSSN+/BCP and PSI electrodes

Photocurrent of DSSN+/COE bilayers were measured weekly on modified gold working electrodes with a BASi potentiostat at room temperature with a working electrode bias of -300 mV, an Ag/AgCl reference electrode, and a Pt-counter electrode (see section 3.5). New electrolyte solution of 10 mM MES pH 6.0, 2 mM 1,1'-dimethyl-4,4'-bipyridinium (methyl viologen, Sigma-Aldrich), 100 µM PMS, 100 µM $K_3[Fe(CN)_6]^{3-}$, and 100 µM $K_4[Fe(CN)_6]^{4-}$. Electrodes were illuminated with 100 µmol m^{-2} s^{-1} (400-700 nm) (approximately 20 mW cm^{-2}) of light from an Oriel Type 1958 tungsten lamp. The electrodes were stored in the dark at 4 ℃ between measurements. Electrodes were tested weekly for 1 to 4 weeks.

3.8 PSI/DSSN+ membrane procedure without BCPs

Cleaned gold electrodes were modified with a solution of 0.075 mM tethering (DPPTE) lipids (10 mM stock in chloroform), 0.075 mM DMPC (10 mM stock in chloroform), and 0.3 mM dithiodiglycolic acid (30 mM stock in 100% ethanol) for one hour to form a self-assembled monolayer (SAM). A solution of 0.5 mM of phosphatidylserine (PS), 25 mol % DSSN+, and 5% octyl-beta-glucoside (OG) was then added to the SAM gold electrodes for 48 hours at 25℃.

To remove OG detergent, a dialysis membrane (10-12 kDa cutoff) was added to the electrode. The gold electrode was clamped with an aluminum clamp to a glass O-ring-joint. The

dialysis membrane was fit to the glass cell opening with a modified dialysis button and secured with an O-ring. The volume of the set-up is 3 mL. Detergent was removed by placing the cell in 1 L of dialysis buffer with a stir bar made from 100 mM NaCl, 50 mM Tris pH 8.3, and 3 mM NaN_3 for 3 days. Dialysis buffer was changed every 24 hours. After 3 days, the dialysis button was removed and deionized water was used to maintain membrane integrity.

Chapter 4

Results and Discussion

The objective of this research was to create a photoconductive PSI-BCP membrane mimicking the natural environment of PSI membrane proteins. Results achieved high membrane photocurrent of 35.0 ± 3.5 μA cm^{-2} without compromising structure. This is approximately twice the photocurrent produced by bio-photovoltaic PSI cells supported by lipid membranes with intercalated COEs, which produce a photocurrent of up to 17.3 ± 1.2 μA cm^{-2}. Longevity testing conducted over a one-month period also showed membrane stability for at least 30 days.

4.1 Block copolymer/PSI/DSSN+ systems produce photocurrent

PSI-BCP bilayer protein systems were placed atop gold electrodes and tested using cyclic voltammetry (CV) to elucidate conductivity atop a gold coated glass electrode. **Figure 10** shows the results of CV for a control bare gold electrode, control BCP layer atop a gold electrode, and for a BCP layer intercalated with the COE, DSSN+, atop a gold electrode. The bare gold electrode shows the most current generation per unit area; however, placing PSI proteins directly onto the electrode surface could damage the protein due to strong interface interactions, resulting in a device with an impractically small lifetime. In comparison, the BCP layer alone on a gold electrode shows some current generation, but it is only enough for minimal electron transfer to the PSI proteins. The BCP layer with intercalated COEs on a gold electrode shows a current generation similar to that of the bare gold electrode, with significant improvement over the BCP layer alone. The addition of the COE allows for enhanced electron transfer from the electrode

through the BCP membrane and prevents the risk of undesirable metal-protein reactions that could damage PSI proteins.

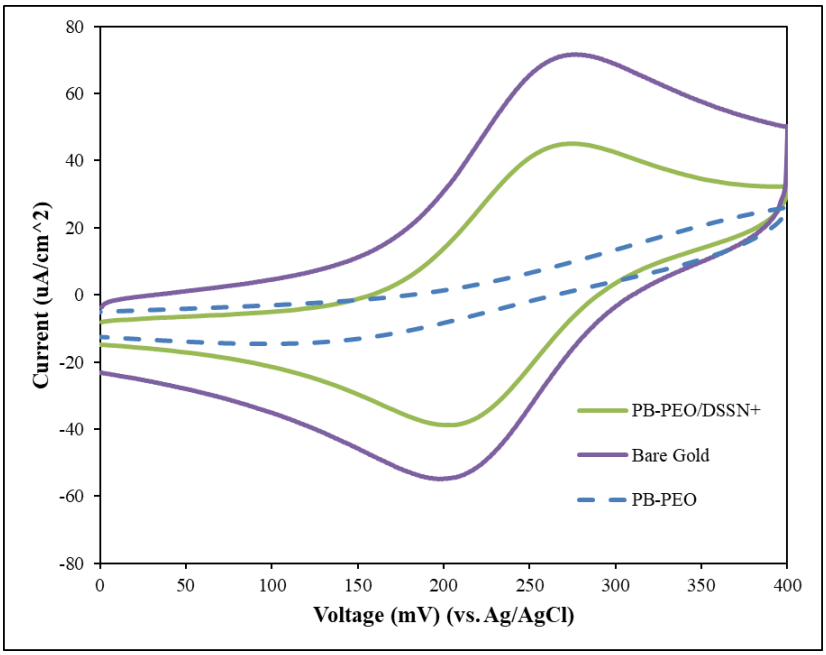

Figure 10. Cyclic voltammetry of modified (PB-PEO/DSSN+ and PB-PEO) and unmodified (bare gold) electrodes.

After testing for conductivity of modified gold electrodes, single time base cyclic voltammetry was used to test the photocurrent of electrodes modified with COE and BCPs, PSI proteins and BCPs, and PSI proteins with BCPs and COEs (**Figure 11**). Electrodes modified with BCPs intercalated with COEs produced the least photocurrent of 0.55 ± 0.13 μA cm^{-2}. Adding PSI proteins to the membrane-electrode interfaces causes a 3.5-fold increase in photocurrent, resulting in a maximum photocurrent of 35 ± 3.5 μA cm^{-2}. Although there is high conductivity through COE intercalated BCP membranes, the slightly negative charge of the PSI membrane proteins provides a contrast to the slightly positively charged BCP-COE membrane system and helps direct electrons through the photovoltaic cell, providing more current through the cell.

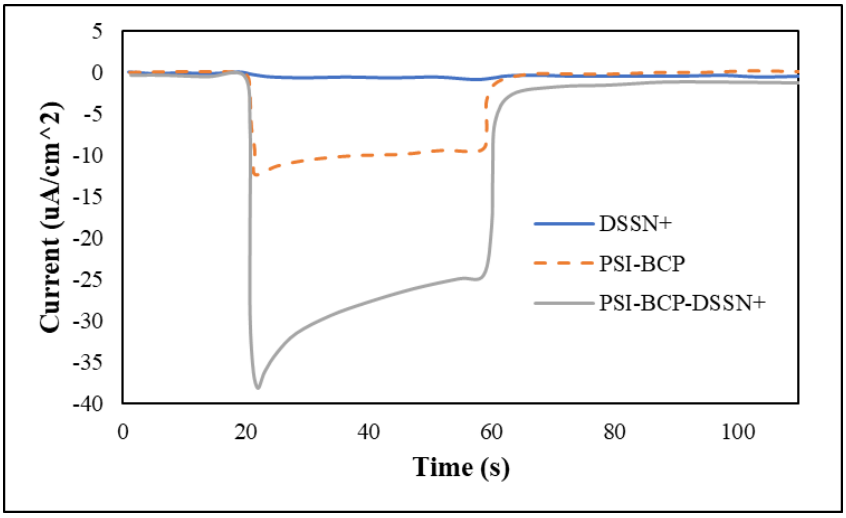

Figure 11. Photocurrent measurements over 40 seconds for modified gold electrodes with and without PSI proteins.

4.2 Block copolymer/PSI/DSSN+ systems maintain stability over time

To test the feasibility of the PSI-BCP membrane systems for commercial use, photovoltaic cells were tested using voltammetry for up to 75 days. Photocurrent measurements remained relatively stable for up to 35 days (**Figure 12A**). Stability testing was conducted weekly for samples up to 35 days, with some additional testing of samples for up to 75 days. Average photocurrent for samples up to 35 days ranged from approximately 0.5 to 0.8 µA cm^{-2}. The average photocurrent over the testing period for each of four samples was also collected, with sample times ranging from 14 to 75 days (**Figure 12B**). The average photocurrent of these samples for long-term study ranged between 0.4 and 0.9 µA cm^{-2}. These results show that the PSI-BCP system tested has a high long-term stability and provides a consistent environment for efficient electron transfer from an electrode surface to native proteins.

Similar devices utilizing PSI proteins for electron transfer range in stability from less than a day to about one year. This highly variable range of longevity depends on many factors

surrounding methods and materials of construction; devices that include more synthetic components tend to have overall longer lifetimes, but do not always provide high photocurrents. The PSI-BCP system at this point has not yet been tested for lifetimes nearing the year marker. However, the reported lifetime of up to 30 days, combined with the high reported photocurrent of approximately 35 µA cm^{-2} is one of the best examples of an organic device with large photocurrent and reasonable stability found in the literature to date.

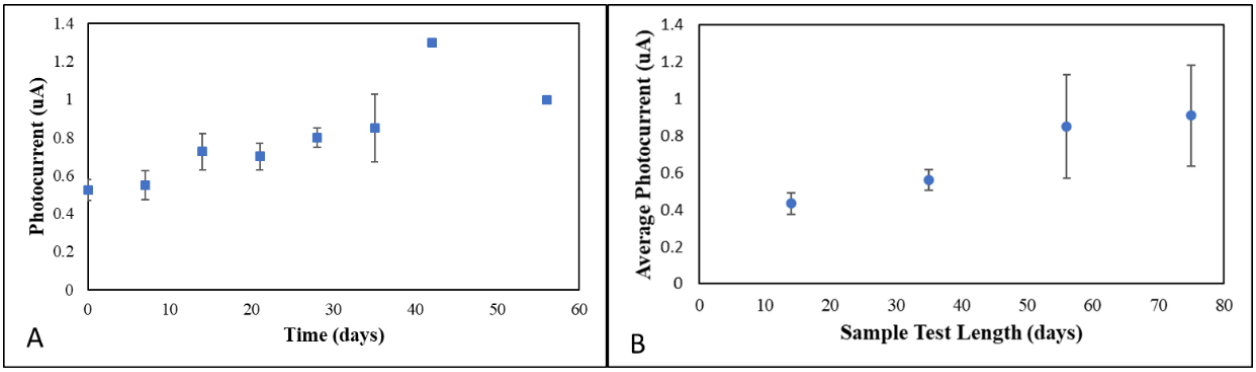

Figure 12. Stability testing for PSI-BCP samples. A. Average photocurrent for each weekly testing period. B. Average photocurrent of each tested sample.

The four devices tested for long term stability maintained an activity between 100% and 60% of their original photocurrent over the 35-day standard testing period. **Figure 13A** shows the photocurrent profile for a sample on its first day of testing, and **Figure 13B** shows the photocurrent profile for the same sample after 35 days. Both of these profiles maintain the same general shape. Although PSI was electrostatically immobilized on the surface of the photovoltaic device, the decrease in overall photocurrent over the study could be a result of loose association

with the electrode. It is possible that over the 35 days, the PSI layer of the device could have been disrupted during the exchange of electrolyte buffer for voltammetry testing.

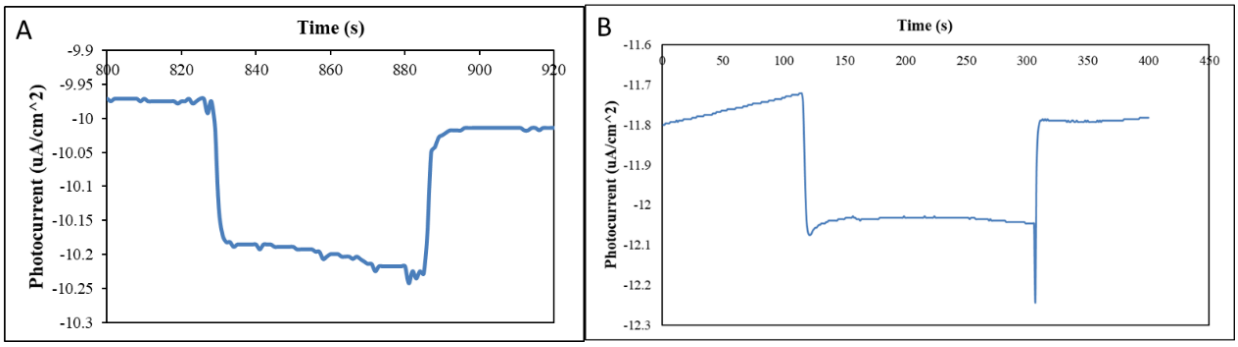

Figure 13. Photocurrent profiles of PSI-BCP organic photovoltaic. A. On day 1 of testing. B. On day 35 of testing.

4.3 Function of PSI proteins is not compromised by block copolymers or DSSN+

Several control experiments were performed to ensure that the functionality of the PSI proteins was not compromised by the addition of the BCPs or the COE, DSSN+. Because PSI proteins function in electron transfer by absorbing light from the surroundings, UV-Vis spectra were taken for PSI with BCPs and PSI in detergent micelles and compared for variation in spectra (**Figure 14**). Any variation would indicate that the ability of PSI proteins to absorb light for use in electron transfer was compromised by their association with BCPs in the system. The overlap of both spectra at major absorbance peaks shows that the BCPs did not influence absorbance properties of the protein. A change in absorbance properties would have likely affected the electron transfer properties of the PSI proteins.

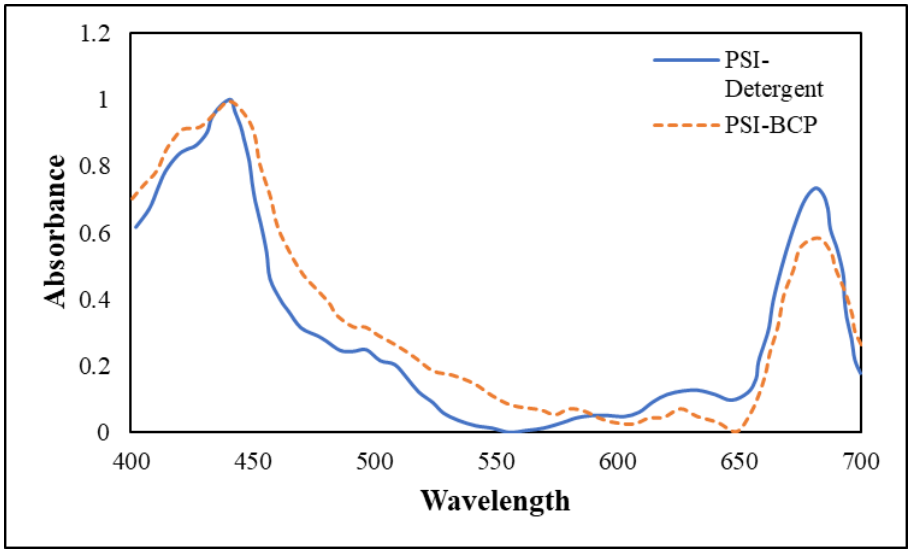

Figure 14. UV-Vis spectra of PSI in detergent micelles or in a BCP membrane.

In order to show that travel of electrons through the COE molecules were the primary method of electron transfer through the membrane, baseline voltammetry testing of BCP molecules without COEs was performed. Membranes were tested using single time-based voltammetry, with light provided to the electrode during the 10-20 second interval and 40-50 second interval (**Figure 15**). It was shown that no photocurrent is produced from BCP membranes without intercalated COEs; as expected the BCP molecules are shown to be electrical insulators requiring the addition of conductive molecules to allow electrons to pass through the membrane. This result shows that all photocurrent was the result of the addition of COEs and PSI to the membrane system.

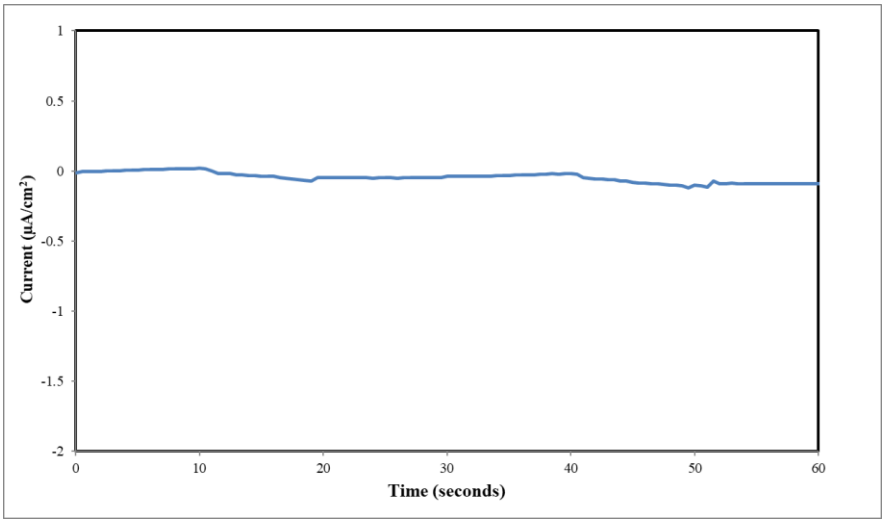

Figure 15. Photocurrent for a BCP membrane without DSSN+.

Finally, to ensure that cross-linking the membrane to provide additional stabilization does not affect the conductivity of the membrae, a UV polymerization reaction was performed on the BCP-COE interface to cross-link the side chains of the polybutadiene polymer within the BCP. Because cross-linking is typically desirable to maintain long term stability of BCP systems, conductivity of cross-linked BCP-COE interfaces were compared to non-crosslinked BCP-COE interfaces (**Figure 16**). It is apparent that cross-linking does not affect the conductivity of the membrane, showing that the BCP-COE membrane material is useful for long-term applications.

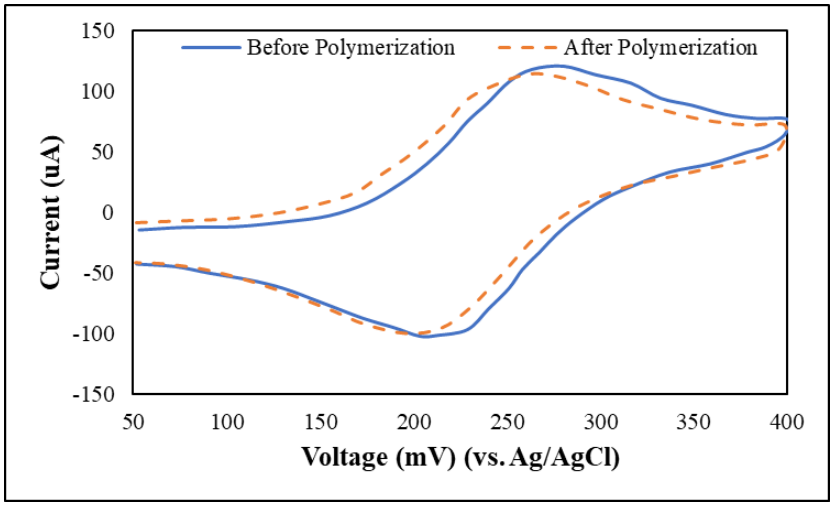

Figure 16. BCP interface with COEs before and after UV polymerization.

Chapter 5

Future Work and Conclusion

The goal of this research was to create a photoconductive PSI-BCP membrane mimicking the natural environment of PSI membrane proteins. Cyclic voltammetry and photocurrent measurements of the PSI-BCP systems showed that the integration of photosystem I proteins with block co-polymers intercalated with conjugated oligoelectrolytes (COEs) does produce large photocurrents of up to 35 ± 3.5 μA cm^{-2}, at minimum a two-fold increase over similar systems which use lipids instead of BCPs. The use of the COE, DSSN+, and the PSI proteins were shown to be the main contributors to electron transfer. DSSN+ makes a large contribution to photocurrent generation through its ability for directed electron transport through membranes, while the slightly negative charge of the PSI protein draws electrons toward the upper layer of the membrane surface away from the slight positive charge of the BCP-COE layers.

This study has shown that natural redox membrane proteins can be incorporated into artificial interfaces, and future work may explore additional redox proteins electrically wired to such artificial interfaces containing block copolymers of different varieties to test the applicability of this method to other systems. This would provide functionality to the membrane system in addition to use in solar energy conversion; for example, the incorporation of hydrogenase proteins may allow for hydrogen production for energy through hydrogen fuel cells, and the use of glucose oxidase enzymes could provide biosensing capabilities within the medical field. Additional tuning procedures may be investigated to enhance the approach for many types of integrated biological-artificial systems. Furthermore, these studies were unable to test the

overall efficiency of the organic photovoltaic as compared to traditional solar devices, nor was the manufacturing cost of such a device explored for commercial use. In particular, photocurrent generation of this experimental device should be tested against a wide range of commercial silicon solar cells at the same conditions. Although some studies report the photocurrent through poly and monocrystalline silicon solar cells to range between 195 and 275 μA cm^{-2},[28] many variables, including wavelength and light intensity can affect the resulting photocurrent of the solar cell, with other studies reporting current densities of microcrystalline silicon cells on the order of 30 mA cm^{-2}.[29] In the future, such testing would provide a better basis for assessing the practicality of using the BCP/PSI device on a large scale for solar energy harvesting. This type of work may be the impetus for the development of a completely artificial bioinspired organic photovoltaic, which would eliminate issues with system stability over several years.

Bibliography

1. McGowan, J. Large-Scale Solar/Wind Electrical Production Systems – Predictions for the 21st Century; In *Energy and the Environment in the 21st Century*; Tester, J. Wood, D. Ferrari, N., Eds.; Cambridge, Mass: MIT Press, 1991.
2. Institute for Energy Research. http://instituteforenergyresearch.org/topics/encyclopedia/renewable-energy (accessed Jan 28, 2018).
3. Growing Market Demand for Renewable Power. http://www.se4all.org/sites/default/files/RE100-Annual-Report2016.pdf (accessed Jan 28, 2018).
4. How Do Solar Panels Work? https://www.livescience.com/41995-how-do-solar-panels-work.html (accessed Jan 28, 2018).
5. Scientists Have Broken the Efficiency Record for Mass-Produced Solar Panels. https://www.sciencealert.com/researchers-have-broken-the-record-for-solar-panel-efficiency-again (accessed Jan 28, 2018).
6. The Average Photovoltaic System Efficiency. https://sciencing.com/average-photovoltaic-system-efficiency-7092.html (accessed Jan 28, 2018).
7. What Happens in Photosystem 1. https://www.enotes.com/homework-help/what-happens-photosystem-1-267873 (accessed Jan 28, 2018).

8. Saboe, P.O.; Lubner, C.E.; McCool, N.S.; Vargas-Barbosa, N.M.; Yan, H.; Chan, S.; Ferlez, B.; Bazan, G.C.; Golbeck, J.H.; Kumar, M. Two-Dimensional Protein Crystals for Solar Energy Conversion. *Adv. Mater.* **2014**. *26*. 7064-7069.
9. Polymer Science Learning Center. http://pslc.ws/macrog/copoly.htm (accessed Jan 28, 2018).
10. Glossary of Nanotechnology and Related Terms. http://eng.thesaurus.rusnano.com/wiki/article613 (accessed Jan 28, 2018).
11. Raguse, B.; Braach-Maksvytis, V.; Cornell, B.A.; King, L.G.; Osman, P.D.; Pace, R.J.; Wieczorek, L. Tethered lipid bilayer membranes: formation and ionic reservoir characterization. *Langmuir*. **1998**. *14*. 648-659.
12. Giess, F.; Friedrich, M.G.; Heberle, J.; Naumann, R.L.; Knoll, W. The protein-tethered lipid bilayer: A novel mimic of the biological membrane. *Biophys. J.*. **2004.** *87*. 3213-3220.
13. Tanaka, M. and Sackmann, E. Polymer-supported membranes as models of the cell surface. *Nature*. **2005**. *437*. 656-663.
14. Won, Y.-Y.; Paso, K.; Davis, H.T.; Bates, F.S. Comparison of Original and Cross-linked Wormlike Micelles of Poly(ethylene oxide-b-butadiene) in Water: Rheological Properties and Effects of Poly(ethylene oxide) Addition. *J. Phys. Chem. B.* **2001**. *105*, 8302-8311.
15. Srinivas, G. ; Shelley, J.C.; Nielsen, S.O.; Discher, D.E.; Klein, M.L. Simulation of Diblock Copolymer Self-Assembly, Using a Coarse-Grain Model. *J. Phys. Chem. B.* **2004**, *108*, 8153-8160.

16. Pata, V. and Dan, N. The Effect of Chain Length on Protein Solubilization in Polymer-Based Vesicles (Polymersomes). *Biophys. J.* **2003**, *85*, 2111-2118.
17. Dittmer, J.J.; Lazzaroni, R.; Leclére, P.; Moretti, P.; Granstrom, M.; Petritsch, K.; Marseglia, E.A.; Friend, R.H.; Brédas, J.L.; Rost, H.; Holmes, A.B. Crystal network formation in organic solar cells. *Sol. Energ. Mat. Sol.* **2000**. *61*. 53-61.
18. Kuang, L.; Olson, T.L.; Lin, S.; Flores, M.; Jiang, Y.; Zheng, W.; Williams, J.C.; Allen, J.P.; Liang, H. Interface for Light-Driven Electron Transfer by Photosynthetic Complexes Across Block Copolymer Membranes. *J. Phys. Chem. Lett.* **2014**. *5*. 787-791.
19. Thurn-Albrecht, T.; DeRouchey, J.; Russell, T.P. Overcoming Interfacial Interactions with Electric Fields. *Macromolecules.* **2000**. *33*. 3250-3253.
20. Tanizake, S. and Feig, M. A generalized Born formalism for heterogenous dielectric environments: application to the implicit modeling of biological membranes. *J. Chem. Phys.* **2005**. *122*. 124706
21. Lee, Y.; Yang, I.; Lee, J.E.; Hwang, S.; Lee, J.W.; Um, S.S; Nguyen, T.L; Yoo, P.J.; Woo, H.Y.; Park, J.; Kim, S.K. Enhanced Photocurrent Generation by Forster Resonance Energy Transfer between Phospholipid-Assembled Conjugated Oligoelectrolytes and Nile Red. *J. Phys. Chem. C*. **2013**. *117*, 3298-3307.
22. Discher, B. M.; Bermudez, H.; Hammer, D. A.; Discher, D.E.; Won, Y-Y.; Bates, F.S. Cross-linked Polymersome Membranes: Vesicles with Broadly Adjustable Properties. *J. Phys. Chem.* **2002.** *106*. 2848-2854.
23. Wang, X.; Liu, G.; Hu, J.; Zhang, G.; Liu, S. Concurrent Block Copolymer Polymersome Stabilization and Bilayer Permeabilization by Stimuli-Regulated "Traceless" Crosslinking. *Angew. Chem. Int. Ed.* **2004**. *126*. 3202-3206.

24. Saboe, P.O; Conte, E.; Chan, S.; Feroz, H.; Ferlez, B.; Farell, M.; Poyton, M.F.; Sines, I.T.; Yan, H.; Bazan, G.C.; Golbeck, J.; Kumar, M. Biomimetic wiring and stabilization of photosynthetic membrane proteins with block copolymer interfaces. *J. Mater. Chem. A.* **2016**. *4*, 15457.

25. Garner, L.E.; Park, J.; Dyar, S.M.; Chworos, A.; Sumner, J.J.; Bazan, G.C. Modification of the Optoelectronic Properties of Membranes via Insertion of Amphiphilic Phenylenevinylene Oligoelectrolytes. *J. Am. Chem. Soc.* **2010**. *132*. 10042-20052.

26. Li, N.; Warren, P.V.; Golbeck, J.H.; Frank, G.; Zuber, H.; Bryant, D.A. Polypeptide composition of the Photosystem I complex and the Photosystem I core protein from *Synechococcus* sp. PCC 6301. *Biochimica et Biophysica Acta (BBA)- Bioenergetics*. **1991**. *1059*. 215-225.

27. Ford, R.C.; Hefti, A.; Engel, A. Ordered arrays of the photosystem I reaction centre after reconstitution: projections and surface reliefs of the complex at 2 nm resolution. *EMBO*. **1990**. *9*. 3067-3075.

28. Perez, E.; Maestro, M.; Garcia, H.; Castan, H.; Duenas, S.; Bailon, L. Presented at the 2013 Spanish Conference on Electron Devices, February 12-14, 2013.

29. Sai, H.; Matsui, T.; Saito, K.; Kondo, M.; Isao, Y. Photocurrent enhancement in thin-film silicon solar cells by combination of anti-reflective sub-wavelength structures and light-trapping textures. *Prog. Photovolt: Res. Appl.* **2015**. *23*. 1572-1580.

ACADEMIC VITA

Emelia Conte
evc5259@psu.edu

Education

The Pennsylvania State University, University Park, PA *May 2018*
BS in Chemical Engineering, minor in Biomedical Engineering
(Honors in Chemical Engineering, The Schreyer Honors College)

Work Experience

Undergraduate Research Assistant *March 2015-May 2018*
Dr. Manish Kumar, The Pennsylvania State University

- Analyzed electron tomographs to elucidate structure of polyamide reverse osmosis (RO) membranes
- Modified RO membranes with methionine to mitigate biofouling
- Produced photosystem I/block-copolymer membranes that generate 40 times more photocurrent than previous systems

Project Engineering Intern *May 2017-August 2017*
Ecolab Inc., Martinsburg, WV

- Managed seven capital projects worth $312,000
- Learned aspects of chemical plant operation, including TPM and project management

Cancer Institute Scholar *June 2013-August 2013*
Magee-Women's Research Institute, Pittsburgh, PA

- Designed procedure to test for treatable protein pathways in breast cancer cell lines
- Preliminarily proved the activation of Wnt/β-catenin pathway in basal breast cancer cell lines

Publications

Biomimetic and bioinspired approaches for wiring enzymes to electrode interfaces
Energy Environ. Sci. 2017, 10, 14.
Biomimetic wiring and stabilization of photosynthetic membrane proteins with block copolymer interfaces
J. Mater. Chem. A. 2016, 4, 15457.

Awards and Grants

2017 Energy and Environmental Science HOT articles
Department of Chemical Engineering Bio Fellowship
NASA Pennsylvania Space Grant Consortium Scholarship Recipient
National Merit Scholarship Corporation Special Scholar Award - PPG

Leadership

Newman Catholic Student Association *August 2014-May 2018*
President, *April 2017- April 2018*; Secretary, *April 2016-April 2017*
Discovery Space Kids Museum *July 2016-May 2018*
Volunteer
Penn State Undergraduate Speaking Center *August 2015-May 2018*
Mentor
Schreyer Honors College Orientation Mentor *August 2016, August 2017*